

Cytotoxicity and solubility evaluation of two types of whiskers by cell magnetometry

Yuichiro Kudo · Yoshiharu Aizawa

Received: 27 August 2010 / Accepted: 3 December 2010 / Published online: 21 January 2011
© The Japanese Society for Hygiene 2011

Abstract

Objectives We investigated two types of whiskers, an antimony-containing tin-oxide-coated aluminum borate whisker (CABW) and an aluminum borate whisker (ABW), which are asbestos substitutes, in order to evaluate the safety of these fibers.

Methods The cytotoxicity and solubility of CABW and ABW were evaluated by cell magnetometry, LDH assay and solubility test.

Results ABW was found to be cytotoxic by cell magnetometry and slightly less soluble than CABW. In addition, it was found that the solubility of both fibers was intermediate between that of chrysotile and rock wool, as compared to our previous test results. Regarding the LDH assay, no significant difference was found among the fibers tested. These findings suggested that CABW, the surface of which is coated with antimony-containing tin oxide, had lower cytotoxicity and slightly higher solubility than ABW.

Conclusions This study was only a short-term cytotoxicity and solubility study. Therefore, further safety assessment should be carried out in long-term experiments to examine the half-life of these fibers and monitor the potential development of lung carcinoma or mesothelioma after intratracheal instillation of these fibers in rats.

Keywords Cell magnetometry · Relaxation · Whisker · Cytotoxicity · Solubility

Introduction

Asbestos has been widely used as an industrial material because of its high fire and heat resistance and chemical stability. Many in vitro and in vivo studies on the hazards of asbestos have been reported [1, 2]. A relationship between asbestos and the development of lung carcinoma and mesothelioma is well documented [3, 4].

In Japan, the use and manufacturing of white asbestos was prohibited in principle in 2004, and a policy to totally ban the use of asbestos by 2008 was established. Taking this trend into consideration, the development and use of asbestos substitutes in industry have been hastened. Currently, many types of man-made mineral fibers have been developed and are widely used as asbestos substitutes, such as building materials and friction materials in brakes. Not only asbestos, but also fibers with a width of less than 0.25 μm and a length greater than 8 μm have been reported to exert especially high carcinogenicity, and fibers of small width, long length and low solubility within the human body may be carcinogenic [5–7].

Whisker, which is a man-made crystalline fiber, is a type of asbestos substitute and is defined as a single crystal with a cross-sectional area of $8 \times 10^{-5} \text{ cm}^2$ or less and a length of 10 times the average cross-sectional diameter or more. Whiskers include aluminum borate whisker, potassium octatitanate whisker (PT) or silicon carbide whisker (SiC). The two types of whiskers, antimony-containing tin-oxide-coated aluminum borate whisker (CABW) and aluminum borate whisker (ABW), used in our study have high intensity, hardness, heat resistance, electrical insulation and chemical resistance. Hence, they are widely used as materials for resin/metal reinforcement, friction, insulation, refractory and heat insulation, etc. Because of such properties, they are expected to be used more extensively in the

Y. Kudo (✉) · Y. Aizawa
Department of Preventive Medicine and Public Health,
Kitasato University School of Medicine, 1-15-1 Kitasato,
Minami, Sagami-hara, Kanagawa 252-0374, Japan
e-mail: yuichiro@med.kitasato-u.ac.jp

future. However, they have been used industrially only recently, with a lower number of safety reports than for other asbestos substitutes. There is therefore an urgent need to evaluate the safety of these whiskers.

In this study, the cytotoxicity of CABW and ABW was evaluated by cell magnetometry and lactate dehydrogenase (LDH) enzyme assay using alveolar macrophages, which play a primary role in the defense mechanism against the invasion of foreign matter in the respiratory tract. Further, solubility was examined using physiological saline or simulated body fluid (Gamble's solution), and compared with that of chrysotile fibers and rock wool (RW) fibers, whose solubility was previously examined in our laboratory [8].

Materials and methods

Test substances

CABW and ABW, both provided by Konica Minolta Business Expert Inc. (Tokyo, Japan), were used as test substances. The mean length of both substances was 10–30 μm and mean width 0.5–1.0 μm . CABW was chemically composed of 60–80% aluminum borate, 16–38% tin oxide, 2–5% titanium dioxide and 2–4% antimony trioxide, and ABW was composed of 97% aluminum borate.

After sterilization by an autoclave (1.1 atmospheric pressure, 121°C, 20 min), these test substances were used after suspension in phosphate-buffered saline (PBS) at pH 7.4.

Alveolar macrophage preparation

Six male Fisher rats (F344/N Slc) weighing 200–250 g were used. Animals were anesthetized by intraperitoneal injection of sodium pentobarbital (100 mg/kg) and killed by exsanguination from the abdominal aorta after making a midline abdominal incision. With the trachea exposed, a silicon tube (Atom Intravenous Catheter, 5 French for cut-down, Atom Medical Corp., Tokyo, Japan) was inserted and fixed. Bronchoalveolar lavage (BAL) was carried out by infusing 4 ml PBS, pH 7.4, containing sterilized 0.1% ethylenediamine tetraacetic acid followed by recovery of the BAL fluid (BALF). This procedure was performed approximately 10 times in total. The BALF obtained was pooled and subjected to centrifugation at 1,800 rpm for 10 min, and the pellet was suspended in serum-free culture medium (Macrophage-SFM liquid, Life Technologies Inc., Rockville, MD). A portion of the suspension was used for determination of cell counts with a hemocytometer after Trypan Blue staining. Cells with a survival rate of 90% or more were used in this study.

The alveolar macrophage suspension prepared by this procedure was diluted with Macrophage-SFM liquid, yielding an aliquot of 1×10^6 cells per well. Each aliquot was poured into a well, with a cell disc of 1 cm diameter.

Cell magnetometry

Cell magnetometry was performed in the same manner as reported by Keira et al. [9]. As an indicator for cell magnetometry, Fe_3O_4 particles suspended in PBS were added at a final concentration of 50 $\mu\text{g}/\text{ml}$ in each well prepared according to the procedure described above. Then, the two test substances were added in the experimental groups at a final concentration of 40, 80 or 160 $\mu\text{g}/\text{ml}$, and 50 μl PBS was added to the negative control group. These test samples were cultured in a 5% CO_2 incubator at 37°C for 18 h. After culturing, the glass disc harboring adherent alveolar macrophages was extracted from each well and placed in a glass weighing bottle containing 1 ml Macrophage-SFM liquid. The samples were subjected to external magnetization for 1/100 s under a magnetizer of a cell magnetometer apparatus. Immediately after that, recording of the remnant magnetic field strength, as measured with a flux-gate-type magnetometer, was started using a pen recorder for 20 min. The apparatus was set to be operated in such a way that the sample table passed over the probe once every 6 s. The temperature was maintained at 37°C by means of a hot-air fan with a thermostat placed beneath the magnetic shield. The curve, which shows the level of relaxation, could be obtained by measuring the remnant magnetic field strength for 20 min post-magnetization. Measurement of the remnant magnetic field strength for 2 min post-magnetization yielded a nearly linear curve when plotted after logarithmic transformation, and the point at which this curve intersected the y -axis was designated B_0 . When expressing the remnant magnetic field immediately after magnetization as B_0 and the decay constant as λ , the remnant magnetic field at t s after termination of external magnetization is represented by the formula $B = B_0 e^{-\lambda t}$, and thus the decay constant (λ) was calculated based on this formula.

LDH assay

In the same way as for cell magnetometry, Fe_3O_4 particles suspended in PBS were added at a final concentration of 50 $\mu\text{g}/\text{ml}$ in each well, followed by addition of the two test samples at a final concentration of 40, 80 or 160 $\mu\text{g}/\text{ml}$ in the experimental group, and 50 μl PBS in the control group. These samples were cultured in a 5% CO_2 incubator at 37°C for 18 h. Then the culture medium was harvested and centrifuged at 1,400 rpm for 5 min to collect the supernatant. Using the supernatant recovered, the quantity

of LDH released into the culture medium was assayed using CytoTox96 Non-Radioactive Cytotoxicity Assay (Promega Corporation, Madison, WI). The amount of LDH release can be assayed by determining the absorbance, since tetrazolium salt is converted to a formazan product that produces a red color. Measurement was performed at absorbance of 492 nm using a microplate reader (MPR-A4, Tosoh Corp., Tokyo, Japan). The amount of LDH released from each test sample was expressed as a % control assuming LDH concentration in the control group was 100%.

Morphological observation

In the electron-microscopic observation, Fe_3O_4 particles were not added. In this investigation, CABW and ABW were added in the experimental groups at a final concentration of 160 $\mu\text{g}/\text{ml}$, and 50 μl PBS was added in the negative control group, followed by culture of cells for 18 h, as described above. Macrophages adsorbed onto the polycationics-treated glass were washed with 0.1 M cacodylate buffer (pH 7.4). Then, following prefixation with 1% glutaraldehyde at 4°C for 3 h and washing, cells were fixed with osmium tetroxide at 4°C for 3 h and washed with cacodylate buffer. For transmission electron microscopic observation, samples thus processed were further subjected to staining, dehydration, resin treatment, embedding, ultrathin slicing with an ultramicrotome and electron staining, followed by evaluation with a model H-600 (Hitachi, Ltd., Tokyo, Japan). For scanning electron microscopic observation, samples were subjected to conductive staining, dehydration, drying and conductive treatment, followed by evaluation with a model S-4500 FE type (Hitachi).

Solubility test

Approximately 0.1 g of each test substance, weighed accurately using an electronic balance, was sandwiched between two pieces of membrane filter of 0.8- μm pore size and 47 mm diameter (Advantec Toyo Kaisha, Ltd., Tokyo, Japan) and set into a filter holder of 47 mm diameter (Advantec Toyo).

In a temperature-controlled room kept at 36°C, physiological saline (pH 7.4; Otsuka Pharmaceutical Co., Ltd., Tokyo, Japan) or Gamble's solution (pH 4.5) (Table 1) was added dropwise at a rate of 0.3 ml/min using an electric pump (MASTER FIE X L/S, Cole-Parmer Instrument Co., Ltd., London, UK), and the filtrate that passed through the filter was pooled in a bottle. The pooled filtrate was recovered every 24 h for 5 consecutive days. This was a flow-type test in which the fluid was always supplied in similar fashion to simulate human exposure. Therefore, the

Table 1 Composition of Gamble's solution

| Chemical substance | Concentration (g/l) |
|---|---------------------|
| Sodium chloride | 12.8297 |
| Disodium hydrogen phosphate | 0.2962 |
| Sodium sulfate | 0.1577 |
| Sodium tartrate | 0.3605 |
| Sodium citrate | 0.3057 |
| Sodium bicarbonate | 5.4058 |
| Sodium lactate | 0.3506 |
| Sodium pyruvate | 0.3437 |
| Glycine | 0.2361 |
| Calcium chloride | 0.5101 |
| Magnesium chloride | 0.4244 |
| Formalin solution (formaldehyde 37%, methanol 8%) | 1 ml |
| Hydrochloric acid | 0.2 ml |

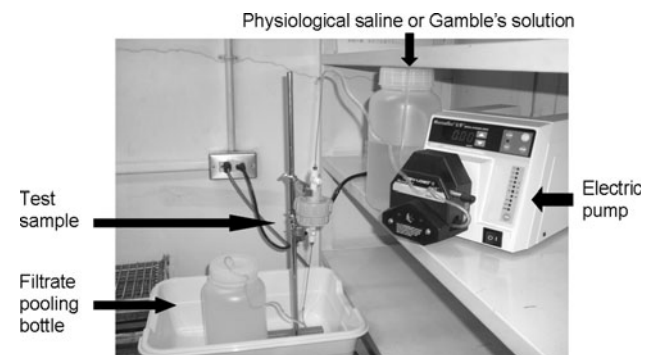


Fig. 1 Experimental apparatus for solubility test

effect of changes in pH and composition of the fluid, which occur as a result of accumulation of reaction products during the dissolving process of the fibers, could be suppressed [5–7]. The elements contained in the recovered filtrate were assayed using an ICP optical spectroscopy instrument (Vista-MPX, Varian Technologies Japan Ltd., Tokyo, Japan), and the dissolution rate constant was calculated (Fig. 1).

Quantitative analysis

Quantitative analyses were performed on elements contained in the filtrate collected every 24 h using an ICP optical spectroscopy instrument.

Preparation of standard solution for standard curve

Standard fluids 1–4 were prepared using ICAL-1 (SPEX CertiPrep Inc., Metuchen, NJ) and a 100-ml volumetric flask. The preparation procedure was as follows:

| | |
|-------------------|---|
| Blank: | 1 ml nitric acid (Kanto Chemical Co., Inc., Tokyo, Japan) |
| Standard fluid 1: | Standard fluid 4 + 1 ml nitric acid |
| Standard fluid 2: | 100 μ l XSTC-760A + 100 μ l ICAL-1 + 1 ml nitric acid |
| Standard fluid 3: | 500 μ l XSTC-760A + 500 μ l ICAL-1 + 1 ml nitric acid |
| Standard fluid 4: | 1,000 μ l XSTC-760A + 1,000 μ l ICAL-1 + 1 ml nitric acid |

The blank and each standard fluid were prepared by adding ultrapure water to make 100 ml.

Preparation of samples

Pretreatment was performed by adding 0.5 ml nitric acid (Kanto Chemical) to 50 ml of each sample.

Analytical method

The standard curve was prepared by the internal standard method using four standard fluids, and quantitative analyses were performed by applying a test sample and yttrium standard stock solution (Kanto Chemical) at the same time.

Dissolution rate constant

The dissolution rate constant was used to evaluate the solubility of fibers. According to the preceding studies, solubility was evaluated taking the surface area of the fiber, which affects solubility, into account [5, 7, 9]. The solubility per unit time and unit surface area, calculated from the axis and the density of fibers, are the dissolution rate constant. The formula is as follows:

$$K = (1 - (M/M_0)^{1/2} D_0 \rho) / 2t$$

where K is the dissolution rate constant ($\text{ng}/\text{cm}^2 \text{ h}$), M_0 the initial fiber mass (mg/l), M the dissolved mass (mg/l), D_0 the initial fiber width (μm), ρ the fiber density (g/cm^3), and t the time (h).

This formula is based on the hypothesis proposed by Stanton et al. [5] that the length of fibers remains unchanged in the dissolving process of fibers, while the width becomes homogeneously thinner. (Fiber density “ ρ ” is presumed to be constant before and after dissolution.)

Statistical analysis

Data of the test substance and the control groups are expressed as mean \pm standard error ($n = 6$). Data were analyzed by one-way analysis of variance using Statview 5.0, and statistical analysis was performed by multiple

comparison using Scheffe’s test. Values of $P < 0.05$ were considered statistically significant.

Results

Cell magnetometry

Relaxation curves were constructed by plotting values of the remnant magnetic field for 20 min after magnetization (Figs. 2, 3). As a result, rapid relaxation was found in the control group. Similarly, rapid relaxation was noted in the CABW-added group. In contrast, a significant delay of relaxation was observed in the 80 and 160 $\mu\text{g}/\text{ml}$ ABW-added groups compared to the control group ($P < 0.05$) (Fig. 3).

The relaxation coefficient during 2-min post-magnetization is shown in Figs. 4 and 5, indicating no marked differences between the CABW-added group and the control group. Compared to the control group, a

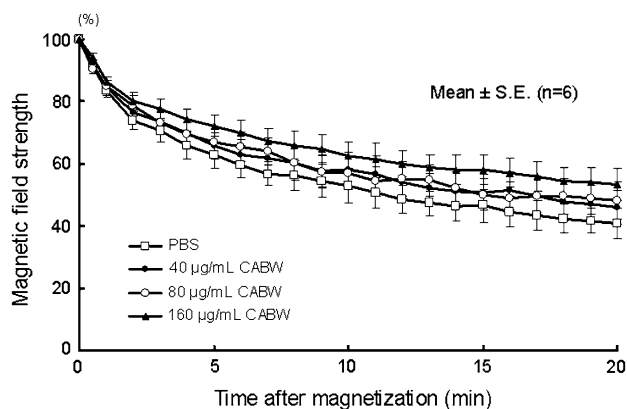


Fig. 2 Relaxation curve of antimony-containing tin-oxide-coated aluminum borate whisker (CABW). Rapid relaxation was found in the PBS- and CABW-added groups

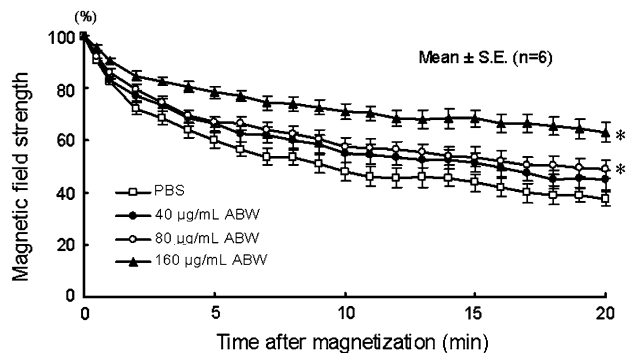


Fig. 3 Relaxation curve of aluminum borate whisker (ABW). Significant delay was found in the 80 and 160 $\mu\text{g}/\text{ml}$ ABW-added groups. $P < 0.05$

significantly lower value was found in the 160 µg/ml ABW-added group ($P < 0.05$) (Fig. 5).

LDH assay

LDH concentration in the supernatant of the alveolar-macrophage culture medium in groups with added test substances is expressed as the percent of that in the control group, as shown in Figs. 6 and 7. No significant difference was found between the control group and the CABW- or ABW-added groups, although there was a trend to an increase with increasing CABW or ABW concentration.

Morphological observation

Morphological observation was carried out using scanning and transmission electron microscopy (TEM and SEM). In the PBS-treated groups, macrophages were round, and the cell surface was entirely covered with numerous microvilli projecting in all directions (Fig. 8a). With the addition of

160 µg/ml CABW or ABW, on the other hand, fibers were seen protruding from the cell surface, and macrophages with a stretched cell membrane appeared to adhere to the fibers (Fig. 8b, c). Transmission electron microscopy demonstrated phagocytic vacuoles, surrounded by a clear membrane structure, in the cytoplasm beneath the microvilli in macrophages in PBS. The nuclei were relatively large with irregular shapes, and smooth-shaped endoplasmic reticulum and lysosomes were seen in the cytoplasm (Fig. 8a). In contrast, projections on the cell surface were reduced in the CABW- or ABW-added groups, and these fibers were absorbed into phagocytic vacuoles, forming vacuoles in the cells. In addition, there was an increase in the number of cells with condensed nuclei (Fig. 8b, c).

Solubility test

The dissolution rate constant of the test substances in physiological saline and Gamble’s solution is shown in

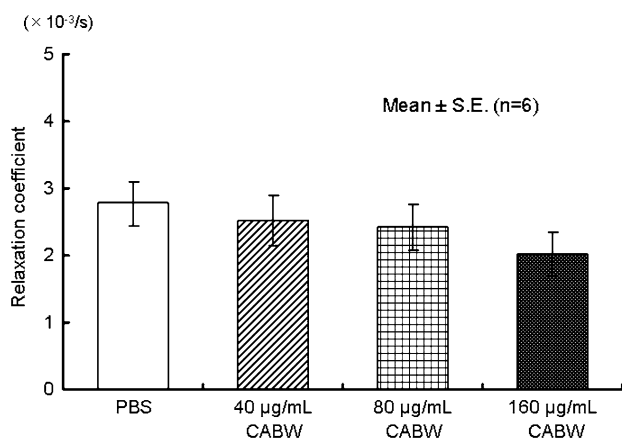


Fig. 4 Relaxation coefficient of CABW. There was no difference between the CABW- and ABW-added groups

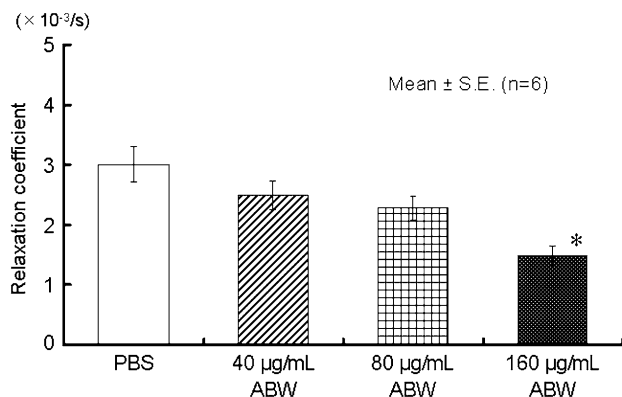


Fig. 5 Relaxation coefficient of ABW. A significantly lower value was found in the 160 µg/ml ABW-added group. $P < 0.05$

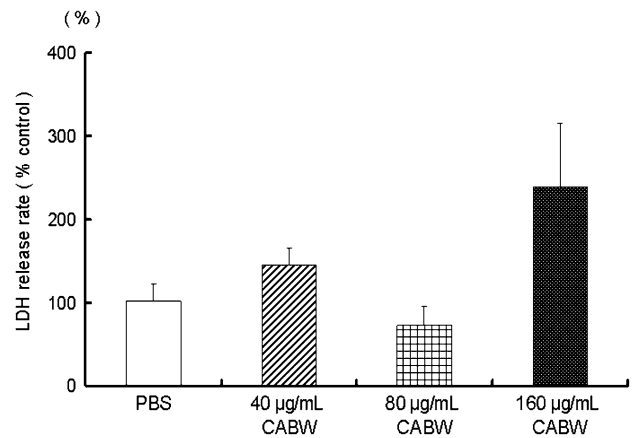


Fig. 6 LDH assay of CABW. No difference was found between the control group and CABW-added group

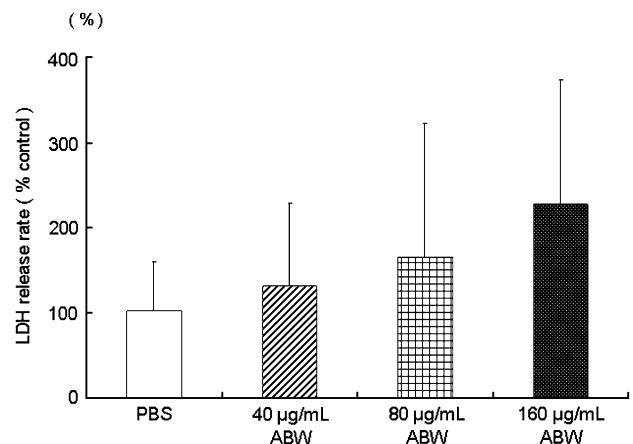


Fig. 7 LDH assay of ABW. No difference was found between the control group and ABW-added group

Fig. 8 Electron microscopic images. **a** (Left) Electron micrograph of a normal macrophage (SEM). The normal macrophage is round, and the cell surface is covered with microvilli projecting in all directions. (Right) Electron micrograph of a normal macrophage (TEM). The nucleus shows an irregular shape. Phagocytic vacuoles, smooth-surfaced endoplasmic reticulum, secretory granules and lysosomes are seen in the cytoplasm. **b** (Left) Electron micrograph of a macrophage in CABW-added group (SEM). Projections on the cell surface were reduced in the CABW-added group. (Right) Electron micrograph of macrophages in CABW-added group (TEM). Projections on the cell surface were reduced in the CABW-added group. **c** (Left) Electron micrograph of macrophages in ABW-added group (SEM). Projections on the cell surface were reduced in the ABW-added group. (Right) Electron micrograph of macrophages in ABW-added group (TEM). Projections on the cell surface were reduced in the ABW-added group

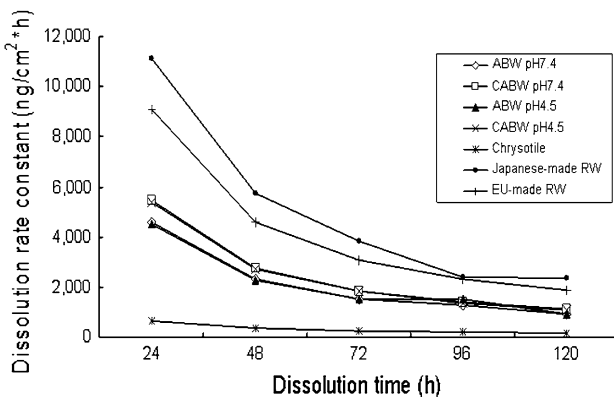
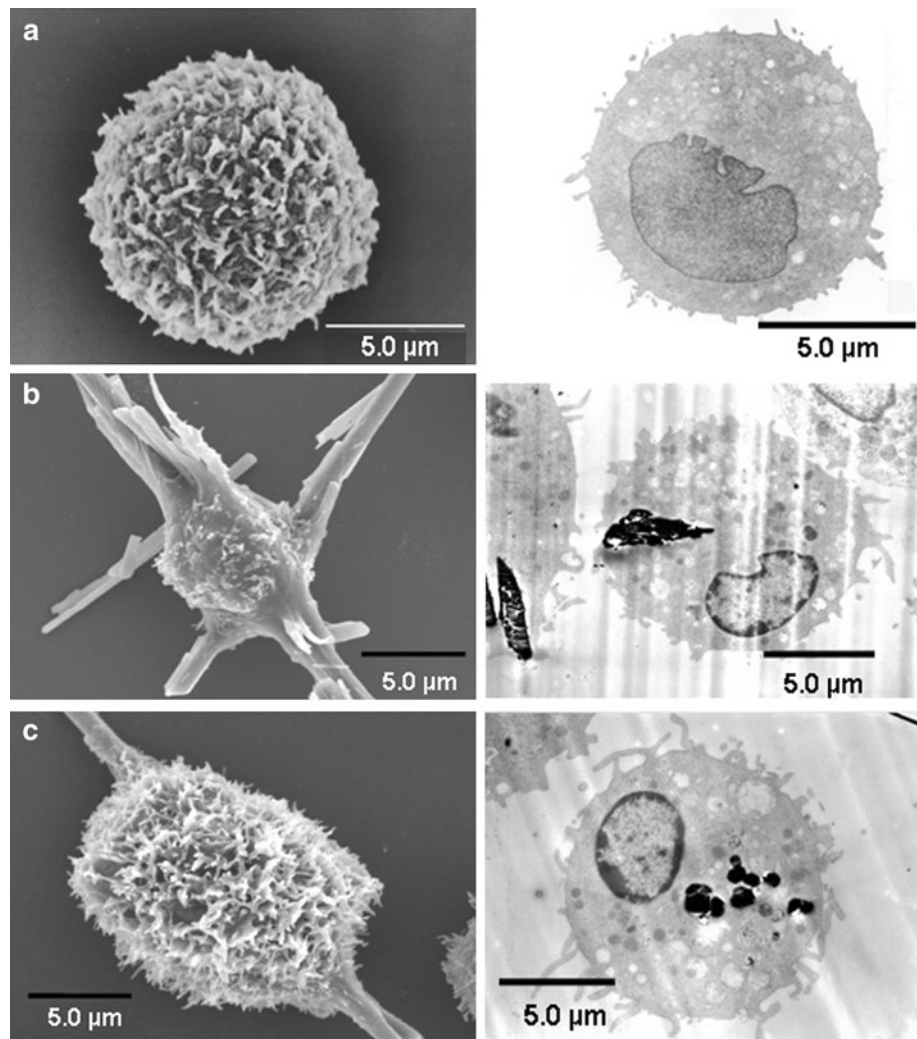


Fig. 9 Dissolution rate constant. The dissolution rate constant of the test substances was higher than that of chrysotile fibers, but lower than that of rock wool

Fig. 9. As for chrysotile fibers and Japanese- and EU-made RW fibers, the dissolution rate constant in physiological saline obtained in the present study is shown as reference.

While the dissolution rate constant of both test substances in physiological saline and Gamble's solution was similar, those of CABW were a little higher than those of ABW. The dissolution rate constant of both test substances was relatively high at 24 and 48 h. In addition, the dissolution rate constant of both test substances in physiological saline was higher than that of chrysotile, but lower than that of RW.

Discussion

Cell magnetometry is an application of lung magnetometry, which was first reported by Cohen [10]. The principle of cell magnetometry is to induce uptake of iron oxide particles by phagocytes and to magnetize these particles by applying external magnetization, followed by measurement of the strength of the remnant magnetic field after cessation of external magnetization, to evaluate the time course of changes in the magnetic field. Rapid

decay of the remnant magnetic field after cessation of magnetization is called relaxation. During external magnetization, magnetic particles become aligned along external magnetic field lines, and after its cessation, these particles start to deviate from their orderly arranged alignment because of their random rotation associated with cytoskeletal motion and translocation of phagocytic vesicles, and, as a result, the remnant magnetic field decays. Brain et al. [11] argued, based on findings obtained in rats, that phagocytosis of iron oxide particles with time took place not as a result of exocytosis of the iron oxide particles, but as a result of their rotation associated with translocation of intracellular organelles. Materials are incorporated in phagocytic vesicles after phagocytosis by macrophages, followed by their digestion. Intracytoplasmic translocation of these phagocytic vesicles and the cytoskeleton (mainly microtubules) are thought to play an important role through their polymerization and depolymerization. The cytoskeleton, which is mainly composed of microtubules, microfilaments and intermediate-diameter filaments, is known to play an important role in maintenance of the cytoplasmic structure, intracellular transport and cellular polarity [12, 13]. It is thought that exposure to harmful substances produces delayed relaxation through their physical and chemical effects on the cytoskeleton [11, 14]. Archer [15] reported that long fibers undergo incomplete uptake because of frustrated phagocytosis in lysosomes and enzyme release, leading to cytotoxicity. Hansen and Mossman [16] reported that the release of superoxide ($O_2^{\cdot-}$) was increased in macrophages containing thin and long fibers with an aspect ratio of 3 or more, and there are many reports on the cytotoxicity of superoxide ($O_2^{\cdot-}$) [17, 18]. Watanabe et al. [19, 20] demonstrated that cell magnetometry showed a concentration-dependent delay of relaxation and a decrease in the relaxation coefficient after addition of PT and SiC to alveolar macrophages, demonstrating the cytotoxicity of PT and SiC. They suggested that incomplete uptake of PT and SiC by cells generated production of oxide, which affected cellular function, leading to a delay of relaxation and a decrease in the relaxation coefficient.

In the present study, no marked difference was found in relaxation and the relaxation coefficient between the CABW-added group and the control group, whereas ABW brought about a dose-dependent delay of relaxation and low relaxation coefficient. The difference between the substances was that the surface of CABW fibers was coated with antimony-containing tin oxide, whereas that of ABW fibers was not. The results of the present study demonstrated that the cytotoxicity evaluated by cell magnetometry of the coated fibers was lower than that of uncoated ones.

In this study, the LDH assay was used for biochemical evaluation. LDH release from the cytoplasm of alveolar macrophages has been used as an indicator of cytotoxicity [21].

PT showed significantly greater LDH release than the control at the same concentration reported in the past [20]. SiC did not induce LDH release in the report by Watanabe et al. [19]; however, it is difficult to compare this result with that of the present study, because the determination method of LDH concentration in the supernatant differed. In LDH assay by the same method as that in the present study in RAW 264.7 cells, PT and SiC showed high LDH release, similarly to crocidolite [22]. In this study, both sample fibers showed no difference compared to the control group, suggesting absence of cytotoxicity.

As mentioned above, electron microscopic observation revealed higher cytotoxicity in the CABW- and ABW-added groups than in the control group.

In the solubility test, CABW tended to have a higher dissolution rate constant than ABW. Intracellular and extracellular pH of macrophages was 4.5 and 7.4, respectively. In a previous study, the dissolution rate constant of SiC in oxalate solution (pH 4.6 and 7.0) was determined by 56-day observation [23]. In that study, the solubility of SiC was low at both pHs and was comparable to that of amosite, a kind of asbestos. The results of that study cannot simply be compared with those of our present study, since the sample fibers and the solution used were different. However, CABW and ABW showed an intermediate dissolution rate constant between those of chrysotile and RW, possibly suggesting poor solubility in the body. The poor solubility suggests that the fibers have high biopersistence, with a possible influence on macrophages and the lung. In particular, the fact that CABW and ABW were slightly soluble in Gamble's solution (pH 4.5) suggests their cytotoxicity to macrophages, which may be related to the delay of relaxation in cell magnetometry and morphological observations by SEM and TEM in our study.

Based on the above findings, ABW showed cytotoxicity in cell magnetometry and showed slightly lower solubility compared to CABW. Both fibers showed intermediate solubility between chrysotile and RW. Thus, CABW, in which the surface of the fibers was coated with antimony-containing tin oxide, showed lower toxicity and slightly higher solubility than ABW. This study was a short-term cytotoxicity/solubility test. Further assessment of safety should be conducted by examining the half-life of fibers and development of lung carcinoma and mesothelioma after intratracheal instillation of these fibers in rats. Moreover, we plan to conduct a DNA ladder detection test to evaluate the possibility of apoptosis as a process of cell death.

References

1. Berry G. Mortality of workers certified by pneumoconiosis medical panels as having asbestosis. *Br J Ind Med*. 1981;38:130–7.
2. Gormley IP, Bolton RE, Brown GM, Davis JM, Wright A. Some observations on the in vitro cytotoxicity of chrysotile prepared by the wet dispersion process. *Environ Health Perspect*. 1983;51:35–9.
3. Churg A, Wright JL, Vedal S. Fiber burden and patterns of asbestos-related disease in chrysotile miners and millers. *Am Rev Respir Dis*. 1993;148:25–31.
4. Mossman BT, Bignon J, Corn M, Seaton A, Gee JB. Asbestos: scientific developments and implications for public policy. *Science*. 1990;274:294–301.
5. Stanton MF, Layard M, Tegeris A, Miller E, May M, Morgan E, et al. Relation of particle dimension to carcinogenicity in amphibole asbestoses and other fibrous minerals. *J Natl Cancer Inst*. 1981;67:965–75.
6. Mohr U, Pott F, Vonnahme FJ. Morphological aspects of mesotheliomas after intratracheal instillations of fibrous dusts in Syrian golden hamsters. *Exp Pathol*. 1984;26:179–83.
7. Pott F, Ziem U, Reiffer FJ, Huth F, Ernst H, Mohr U. Carcinogenicity studies on fibers, metal compounds, and some other dusts in rats. *Exp Pathol*. 1987;32:129–52.
8. Kudo Y, Aizawa Y. Biopersistence of rock wool in lungs after short-term inhalation in rats. *Inhal Toxicol*. 2008;20:139–47.
9. Keira T, Okada M, Katagiri H, Aizawa Y, Okayasu I, Kotani M. Magnetometric evaluation for the effect of chrysotile on alveolar macrophages. *Tohoku J Exp Med*. 1998;186:87–98.
10. Cohen D. Ferromagnetic contamination in the lungs and other organs of the human body. *Science*. 1973;180:745–8.
11. Brain JD, Bloom SB, Valberg PA. Magnetometry: a tool for studying the cell biology of macrophages. In: Atsumi K, Kotani M, Ueno S, Katila T, Williamson SJ, editors. *Bio-magnetism'87*. Tokyo: Tokyo Denki University Press; 1988. p. 10–7.
12. Cassimeris L. Regulation of microtubule dynamic instability. *Cell Motil Cytoskeleton*. 1993;26:275–81.
13. Maccioni RB, Combiato V. Role of microtubule-associated proteins in the control of microtubule assembly. *Physiol Rev*. 1995;75:835–64.
14. Nemoto I, Ogura K, Toyotama H. Estimation of the energy of cytoplasmic movements by magnetometry: effects of temperature and intracellular concentration of ATP. *IEEE Trans Biomed Eng*. 1989;36:598–607.
15. Archer VC. Carcinogenicity of fibers and films: a theory. *Med Hypotheses*. 1979;5:1257–62.
16. Hansen K, Mossman BT. Generation of superoxide (O_2^-) from alveolar macrophages exposed to asbestiform and nonfibrous particles. *Cancer Res*. 1987;47:1681–6.
17. Williams AJ, Cole PJ. In vitro stimulation of alveolar macrophage metabolic activity by polystyrene in the absence of phagocytosis. *Br J Exp Pathol*. 1981;62:1–7.
18. Kennedy TP, Dodson R, Rao NV, Ky H, Hopkins C, Baser M, et al. Dusts causing pneumoconiosis generate OH and produce hemolysis by acting as Fenton catalysts. *Arch Biochem Biophys*. 1989;269:359–64.
19. Watanabe M, Okada M, Aizawa Y, Sakai Y, Yamashina S, Kotani M. Magnetometric evaluation for effects of silicon carbide whiskers on alveolar macrophages. *Ind Health*. 2000;38:239–45.
20. Watanabe M, Shibata K, Okada M, Kudo Y, Niitsuya M, Satoh T, et al. Magnetometric evaluation for cytotoxicity of potassium octatitanate whisker on alveolar macrophage of Fischer 344 rats. *J Occup Health*. 2002;44:321–8.
21. Wroblewski F, Ladue JS. Lactic dehydrogenase activity in blood. *Proc Soc Exp Biol Med*. 1955;90:210–3.
22. Ishihara Y, Kohyama N, Nagai A, Kagawa J. Cellular biological effects and a single transtracheal injection test in three types of whisker fibers. *Inhal Toxicol*. 1998;10:275–91.
23. Searl A, Buchanan D, Cullen RT, Jones AD, Miller BG, Soutar CA. Biopersistence and durability of nine mineral fibre types in rat lungs over 12 months. *Ann Occup Hyg*. 1999;43:143–53.